A GHz operating ScAlN based SAW resonator used for Surface Acoustic Waves/Spin Waves Coupling

I. Zdru[1], C. Nastase[1], L. N. Hess[2], F. Ciubotaru[3], A. Nicoloiu[1], D. Vasilache[1], M. Dekkers[4], M. Geilen[2], C. Ciornei[1], A. Dinescu[1], C. Adelmann[3], M. Weiler[2], P. Pirro[2] and A. Müller[1]

[1] IMT-Bucharest, 077190, Romania (e-mail: alexandru.muller@imt.ro)
[2] Fachbereich Physik and Landesforschungszentrum OPTIMAS, Technische Universität Kaiserslautern, 67663, Germany (e-mail: ppirro@rhrk.uni-kl.de)
[3] F. Ciubotaru and C. Adelmann are with IMEC, Leuven B-3001, Belgium (e-mail: florin.ciubotaru@imec.be)
[4] M. Dekkers is with SOLMATES, Enschede, 7521, Netherlands (e-mail: matthijn.dekkers@solmates-pld.com)

Abstract—A thin ScAlN layer was deposited on high resistivity (111) oriented silicon and two port surface acoustic wave (SAW) devices were manufactured, using advanced nanolithographic techniques, on this material. The Surface Acoustic Wave and Spin Wave (SAW/SW) coupling was performed via a thin magnetostrictive layer (Ni) placed between the interdigitated transducers (IDTs) of the SAW device. Since the phase velocity in this material is lower than in the Si substrate, both Rayleigh (4.67 GHz) and Sezawa (8.05 GHz) propagation modes could be observed. The amplitude of the S_{21} parameter around the two resonances was measured for values of the magnetic flux density (B) from -280 to +280 mT, at different angles (θ) between the SAW propagation direction and the magnetic field direction. A maximum decrease of 2.54 dB occurred in S_{21} for the Rayleigh mode at $\mu_0 H$ = -90 mT, and of 7.24 dB for the Sezawa mode at $\mu_0 H$ =-203 mT, both at θ = 45°. These values were extracted from time gated processing of the frequency domain raw data.

Index Terms—Sc doped AlN, surface acoustic waves, spin waves, magnetic field, Rayleigh mode, Sezawa mode

INTRODUCTION

The interaction of acoustic waves and magnetic excitations (magnons, spin waves) through magnetoelasticity was proposed in the late 50s, by Kittel [1]. The past few years have seen a clear revival of the topic related to acoustic wave excitation of spin waves focusing on potential applications in the field of spintronics or magnonics, as a thin ferromagnetic (FM) layer deposited between the two interdigital transducers (IDTs) of a modern surface acoustic wave (SAW) device can be used to couple SAWs with spin waves (SW). The spin manipulation and control via SAWs can have a major impact in future quantum computing applications. The coupling of acoustic waves with spin waves (SAW/SW coupling) represents a possible direction in the manufacturing of hybrid spin wave–CMOS circuits that can be integrated alongside CMOS circuits.

The mechanism of SAW/SW coupling is analyzed using the Landau-Lifschitz-Gilbert equation [2], [3]. One of the origins of non-reciprocal SAW/SW coupling stems from the Interfacial Dzyaloshinskii-Moriya Interaction (IDMI) [4], [5], an interaction induced at the interface of a heavy metal layer (e.g. Pt) in contact with a FM layer which leads to a non-reciprocal spin wave dispersion. Nonreciprocity of SAW/SW coupling also appears irrespective of IDMI, due to the elliptical polarization of SAWs and SWs, as recently demonstrated in [6].

The spin-wave resonance has previously been acoustically excited, e.g., by a SAW propagating in 50 nm thin Ni layer [7] respectively Co/Pt 10/7 nm bilayer [8] placed between the IDTs of the SAW device with fingers/interdigit spacing 5 μm wide, in the presence of a magnetic field. The 9th harmonic, at 1.54 GHz, has been used. Spin wave generation by SAW was experimentally evidenced by Sasaki in 2017 [9] using the 13th harmonic resonance around 2.2 GHz. Recently, the interaction of SAWs with SW in thin Ni films was demonstrated using the 5th harmonic of the Rayleigh mode, at 4.5 GHz [10].

These works which demonstrate the SAW/SW coupling have used lithium niobate (LN), [7], [8], [9] and lithium tantalite (LT) [10] as piezoelectric material, for SAW devices manufacturing. Because of the relative low value for the fundamental resonance frequency (usually < 200 MHz for LN and < 1 GHz for LT) obtainable from the Rayleigh mode, high order and usually lower amplitude harmonics need to be used in order to fit the SAW resonance to the

spin wave resonance (SWR). This can reduce the coupling efficiency.

The most common piezoelectric materials for SAW devices manufacturing are quartz, LN and LT, intensively used nowadays in mobile phone applications. Although they have excellent piezoelectric properties, the fundamental operation frequency of filters manufactured on these materials is limited to maximum 2-2.5 GHz, due to line-width size limitations imposed by their surface quality. These limited frequencies are not high enough for many novel applications in communications, sensors and also SAW/SW coupling.

In order to increase the resonance frequency of the SAW devices, layered structures, such as III-nitride wide-bandgap thin films semiconductors (deposited or grown on Si or SiC substrates), that allow advanced nanolithographic processes on their top surface, are of high interest. SAW resonators manufactured on GaN/Si and AlN/Si layered structures with resonance frequencies above 5 GHz, and high sensitivity sensors based on them have been reported in the last years [11], [12], [13]. ScAlN is a novel material and a great candidate for acoustic devices fabrication, due to its excellent piezoelectric properties: high phase velocity, high coupling coefficient, k^2_{eff}, high Q-factor, high values of piezoelectric constants, surpassing the reported values for other group III-nitrides [14], [15].

It is the purpose of this paper to demonstrate the interaction between surface acoustic waves and spin waves in a thin magnetic layer placed between the IDTs of SAW device manufactured on ScAlN/Si. Similar to [7] the decrease of the amplitude of the SAW transmission as function of the magnetic flux density, is used to evidence the SAW/SW coupling.

ScAlN DEPOSITION, DEVICE FABRICATION AND CHARACTERIZATION

A 800 nm thin layer of ScAlN (30% Sc doped) was deposited on high resistivity (ρ >10 kΩ·cm) <111> oriented Si wafers, using Solmates Pulsed Laser Deposition Equipment (SMP-800). The surface temperature of the wafer was kept close to 400°C. By optimizing process parameters, the ScAlN thin film stress was tuned to 0 MPa (stress neutral). Theta-2theta XRD spectrum shows single oriented <002> wurtzite ScAlN (at 36.2°) on Si wafers (Fig.1 left). A good texture quality on the Si substrate is observed from the Full Width at Half Maximum of the rocking curve (Fig.1 right), which is about 2.5°.

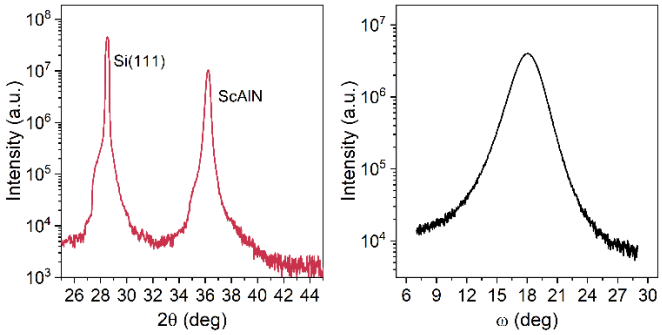

Fig. 1. XRD diagram for the ScAlN films grown on Si <111> (left) and the Rocking curve corresponding to ScAlN (right).

SAW devices, with a magnetostrictive layer placed between the two IDTs have been patterned on the ScAlN/Si wafer (see Fig. 2). First, the coplanar waveguide ports were patterned; conventional photolithography, e-gun metallization (Ti/Au 10/40 nm) and lift-off technique have been used. The SAW devices have 170 nm wide IDTs (75 pairs of fingers/spacings and 50 reflectors) developed by e-beam lithography. The IDTs were deposited by e-gun evaporation (Ti/Au 5/45 nm) and selectively removed by lift-off process. The distance between the IDTs was 200 µm. A Ti/Au overlay (10/300 nm) deposition was performed, to ensure the continuity of the metallization. Finally, a magnetostrictive layer (Ni/Au 12/3 nm) having 140 µm × 166 µm was deposited and centered between the IDTs by lift-off. The 3 nm thin Au layer protects Ni from native oxidation (Fig. 2). The structure is similar to those recently presented by the authors in [16].

On this wafer, S parameter measurements (Fig. 3) revealed two resonance frequencies: at 4.67 GHz, the Rayleigh (R) mode and at 8.05 GHz, the Sezawa (S) mode. The S mode appears in „slow on fast" structures when the phase velocity in the overlayer (ScAlN with 30% Sc) is lower than its value in the substrate (Si) [14], [17] and exhibits higher resonance frequency than the R mode, for the same IDT design.

The k^2_{eff} and the phase velocity (v_{ph}) were calculated, according to the formulas from [18], and the Q factor according to the formula $Q=f_{res}/3dB$ bandwidth, for both resonance frequencies; results are presented in Table 1. The phase velocities obtained for the R and S modes are in good agreement with other reported values for ScAlN [19],

[20].

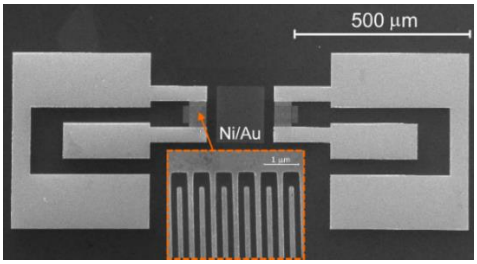

Fig. 2. SEM photos of the two-ports SAW device with a magnetostrictive layer placed between the two IDTs

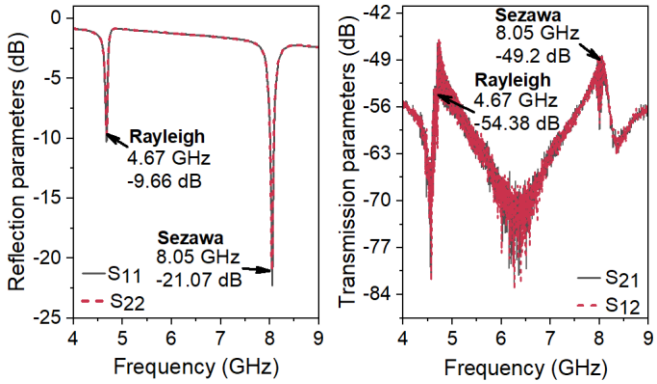

Fig. 3. Measured reflection (left) and transmission parameters (right) of the two-ports manufactured SAW devices

TABLE I
MEASUREMENT RESULTS FOR THE ANALYZED SAW DEVICE

	f_{res} (GHz)	Q	k^2_{eff} (%)	v_{ph} (m/s)
R	4.67	137	4.2	3175
S	8.05	403	5.2	5474

COUPLING OF SURFACE ACOUSTIC WAVES WITH SPIN WAVES

In order to observe the SAW/SW coupling, the SAW structures are placed on a special rotating holder (Fig. 4a), so different angles between the magnetic field and the SAW propagation direction can be established. Furthermore, the holder is placed in an in-house built setup for S parameters measurements (Fig.4b), introduced in a cryostat from Janis (which ensures a controlled temperature and pressure during measurements). The cryostat can be placed between the two poles of an electromagnet (Fig. 4c).

Frequency domain (FD) raw measurements and time gated data processing have been performed. Time gated data processing is necessary in magnetic SAW measurements, especially at frequencies beyond 1 GHz, in order to separate the SAW transmission from electromagnetic cross talk and triple transit effects [21], [22]. Results are summarized in Figs. 5& 6.

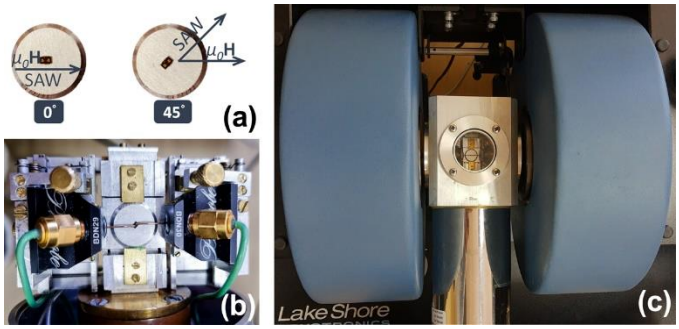

Fig. 4. Measurement set-up: the device on a rotating holder (a); in-house built setup for cryostat microwave measurements (b); the SAW structure in the cryostat, placed in magnetic field (c)

Fig. 5 shows the measured S_{21} vs. frequency, at $\theta = 45°$, for the Rayleigh (left) and respectively Sezawa mode (right), for two different values of the applied magnetic field strength, μ_0H: the reference value, -280 mT, where there is no influence of the magnetic field on S_{21}, and the value where the maximum absorption was observed (-90 mT for Rayleigh and -203 mT for the Sezawa mode). We observe a maximum decrease of 2.54 dB in S_{21} for the Rayleigh mode and 7.24 dB for the Sezawa mode from time gated processing of the raw FD data. Similar curves have been obtained for-$\theta = 0$, 10, 25 and 35°.

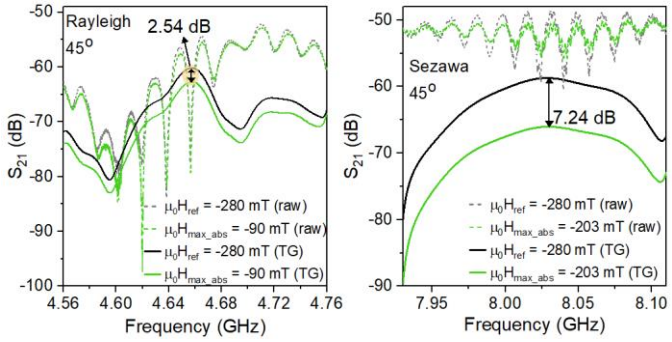

Fig. 5. S_{21} measured at the initial μ_0H_{ref} (dashed black curve) and at B$\mu_0H_{max_abs}$, the value where the maximum absorption was observed (dashed green curve) for Rayleigh (left) and Sezawa (right) modes; solid curves resulted from time gated-(TG) data processing.)

A measure for the energy transfer from SAW to SW can be obtained by using the modulus of the difference between the values of S_{21} at resonance for each applied magnetic field (μ_0H_n) from -280 mT to +280 mT and the value of S_{21} at resonance for the initial applied magnetic field (μ_0H_{ref}), $\Delta S_{21} = |S_{21}{}^{\mu_0H_n} - S_{21}{}^{\mu_0H_{ref}}|$. Fig 6. presents ΔS_{21} vs. B, for all measured angles both for the Rayleigh mode (Fig. 6a) and the Sezawa mode (Fig. 6b) (time gated processed data). It is evident that the effect of energy transfer from the SAW to the SW is stronger for the Sezawa mode and the maximum effect appears at $\theta = 45°$; the effect is strongly suppressed for $\theta = 0°$. The values of ΔS_{21} for the Sezawa mode exceed the values reported by previous works on LN [6], [7]. A fair comparison would need to take into account the length of the FM film (w_{FM}) in the propagation path by referring to $\Delta S_{21}/w_{FM}$ [6]. In the present work $w_{FM} = 140$ μm is smaller than other reported FM film lengths (> 750 μm) [6], [7] and $\Delta S_{21}/w_{FM}$ is about 2 times higher for the Rayleigh mode. The value of μ_0H where the maximum absorption is observed is independent on θ, indicating weak magnetic anisotropy of the Ni film [23].

Also, nonreciprocity is evident in Fig. 6 a, b, as the value of ΔS_{21} is higher for resonances at negative values of μ_0H than for positive ones, for both R and S modes for all measured angles. Fig 6 c presents $\gamma_{R,S}=\Delta S_{21}(-\mu_0H)/\Delta S_{21}(+\mu_0H)$ vs. $|\mu_0H|$ (which is a measure of nonreciprocity) for values of μ_0H around the resonance, for both propagation modes. We can observe that γ decrease monotonic with the angle and is higher for the S mode than for the R mode.

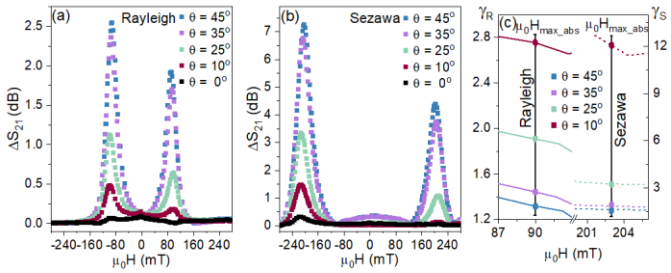

Fig. 6. ΔS_{21} vs $\mu_0 H$ for Rayleigh (a) and Sezawa (b) modes for different values of θ. $\gamma_{R,S}=\Delta S_{21}(-\mu_0 H)/\Delta S_{21}(+\mu_0 H)$ vs $|\mu_0 H|$ around resonance (c).

CONCLUSION

SAW/SW coupling was demonstrated with GHz operating SAW devices manufactured on ScAlN/Si using the fundamental Rayleigh resonance at 4.67 GHz and also the fundamental Sezawa mode resonance at 8.05 GHz. For a magnetostrictive Ni film of 15 nm thickness, the maximum values were obtained for ΔS_{21} when θ = 45° - 2.54 dB (R mode) respectively 7.24 dB (S mode), the last one exceeding the values reported up to now on LN. These devices demonstrate the fit of the fundamental Rayleigh and Sezawa resonance frequencies with the SW resonances, an impossible task for LN, where high order and lower amplitude harmonics are used. Furthermore, in contrast to LN and LN, ScAlN/Si has the major advantage to be CMOS compatible. Future work will be focused on a detailed analysis of nonreciprocity as well as on optimization of the ScAlN/Si SAW structures for SAW/SW coupling, including alternative magnetostrictive metallization.

REFERENCES

[1] C. Kittel, "Excitation of spin waves in a ferromagnet by a uniform rf field", *Physical Review*, vol. 110, no. 6, pp. 1295–1297, 1958, https://doi.org/10.1103/PhysRev.110.1295.

[2] T. L. Gilbert, "A phenomenological theory of damping in ferromagnetic materials," *IEEE Trans. Magn.*, vol. 40, no. 6, pp. 3443–3449, 2004, 10.1109/TMAG.2004.836740.

[3] L. D. Landau and E. M. Lifshitz, "On the theory of the dispersion of magnetic permeability in ferromagnetic bodies" *Perspectives in Theoretical Physics*, pp. 51-65, 1992, https://doi.org/10.1016/B978-0-08-036364-6.50008-9

[4] R. Verba, I. Lisenkov, I. Krivorotov, V. Tiberkevich, A. Slavin, "Nonreciprocal Surface Acoustic Waves in Multilayers with Magnetoelastic and Interfacial Dzyaloshinskii-Moriya Interactions", *Physical Review Applied*, vol. 9, Issue 6, 064014, 2018

[5] T. Böttcher, K. Lee, F. Heussner, S. Jaiswal, G. Jakob, M. Kläui, B. Hillebrands, T. Brächer, P. Pirro "Heisenberg Exchange and Dzyaloshinskii–Moriya Interaction in Ultrathin Pt (W)/CoFeB Single and Multilayers", *IEEE Transactions on Magnetics*, vol. 57, no. 7, pp. 1-7, 2021, 10.1109/TMAG.2021.3079259.

[6] M. Küss, M. Heigl, L. Flacke, A. Hörner, M. Weiler, M. Albrecht, A. Wixforth "Nonreciprocal Dzyaloshinskii-Moriya Magnetoacoustic Waves" *Phys. Rev. Lett.*, vol. 125, no. 21, p. 217203, 2020, https://doi.org/10.1103/PhysRevLett.125.217203

[7] M. Weiler, L. Dreher, C. Heeg, H. Huebl, R. Gross, M.S. Brandt, S.T.B. Goennenwein, "Elastically driven ferromagnetic resonance in nickel thin films", *Phys. Rev. Lett.*, vol 106, no.11, 117601, 2011 https://doi.org/10.1103/PhysRevLett.106.117601 .

[8] M. Weiler, H. Huebl, F.S. Goerg, F.D. Czeschka, R. Gross, S.T.B. Goennenwein, "Spin pumping with coherent elastic waves", Phys. Rev. Lett., vol. 108, no. 17, 176601, 2012, https://doi.org/10.1103/PhysRevLett.108.176601 .

[9] R. Sasaki, Y. Nii, Y. Iguchi, Y. Onose, "Nonreciprocal propagation of surface acoustic wave in Ni/LiNbO3", Phys. Rev. B., vol. 95, no.2, 020407, 2017, https://doi.org/10.1103/PhysRevB.95.020407 .

[10] M. Küss, M. Heigl, L. Flacke, A. Hefele, A. Hörner, M. Weiler, M. Albrecht, and A. Wixforth "Symmetry of the Magnetoelastic Interaction of Rayleigh and Shear Horizontal Magnetoacoustic Waves in Nickel Thin Films on $LiTaO_3$", Phys. Rev. Applied vol. 15, Issue 3, 034046, 2021, https://doi.org/10.1103/PhysRevApplied.15.034046 .

[11] A. Müller, D. Neculoiu, G. Konstantinidis, G. Deligeorgis, A. Dinescu, A. Stavrinidis, A. Cismaru, M. Dragoman, A. Stefanescu, "SAW devices manufactured on GaN/Si for frequencies beyond 5 GHz", *Electron Devices Lett*, vol. 31, no. 12, pp. 1398-1400, 2010, 10.1109/LED.2010.2078484.

[12] A. Müller, G. Konstantinidis, V. Buiculescu, A. Dinescu, A. Stavrinidis, A. Stefanescu, G Stavrinidis, I Giangu, A Cismaru, A Modoveanu, "GaN/Si based single SAW resonator temperature sensor operating in the GHz frequency range" *Sens Actuators A Phys.*, vol 209, pp. 115-123, 2014, https://doi.org/10.1016/j.sna.2014.01.028 .

[13] A. Nicoloiu, G.E. Stan, C. Nastase, G. Boldeiu, C. Besleaga, A. Dinescu, A. Müller, "The Behavior of Gold Metallized AlN/Si- and AlN/Glass-Based SAW Structures as Temperature Sensors", IEEE Trans Ultrason Ferroelectr Freq Control, vol. 68, no. 5, pp. 1938-1948, 2021, 10.1109/TUFFC.2020.3037789.

[14] F. Hadj-Larbi, R. Serhane, "Sezawa SAW devices: Review of numerical-experimental studies and recent applications" Sens Actuators A Phys, vol. 292, pp. 169-197, 2019, https://doi.org/10.1016/j.sna.2019.03.037

[15] B. Lin, Y. Liu, Y. Cai, J. Zhou, Y. Zou, Y. Zhang, C. Sun, "A High Q Value ScAlN/AlN-Based SAW Resonator for Load Sensing", *IEEE Trans. Electron Devices*, vol. 68, no. 10, pp. 5192-5197, 2021, 10.1109/TED.2021.3107232.

[16] A. Nicoloiu, C. Nastase, I. Zdru, D. Vasilache, G. Boldeiu, M. C. Ciornei, A. Müller, "Novel ScAlN/Si SAW-type devices targeting surface acoustic wave/spin wave coupling", *IEEE International Semiconductor Conference (CAS)*, Sinaia, Romania, 2021, pp. 67-70, 10.1109/CAS52836.2021.9604142.

[17] A. Müller, I. Giangu, A. Stavrinidis, A. Stefanescu, G. Stavrinidis, A. Dinescu, G. Konstantinidis, "Sezawa Propagation Mode in GaN on Si Surface Acoustic Wave Type Temperature Sensor Structures Operating at GHz Frequencies", *IEEE Electron Device Lett*., vol. 36, pp. 1299–1302, 2015, 10.1109/LED.2015.2494363.

[18] M. Park, Z. Hao, D. G. Kim, A. Clark, R. Dargis, A. Ansari, "A 10 GHz single-crystalline scandium-doped aluminum nitride Lamb-wave resonator", *20th International Conference on Solid-State Sensors, Actuators and Microsystems & Eurosensors XXXIII (TRANSDUCERS & EUROSENSORS XXXIII),* Berlin, Germany, 2019, pp. 450-453, 10.1109/TRANSDUCERS.2019.8808374.

[19] M. Park, Z. Hao, R. Dargis, A Clark, A. Ansari, "Epitaxial aluminum scandium nitride super high frequency acoustic resonators" *Journal of Microelectromechanical Systems*, vol 29, no. 4, pp. 490-498, 2022, 10.1109/JMEMS.2020.3001233.

[20] H. Liu, Q. Zhang, X. Zhao, F. Wang, M. Chen, B. Li, S. Fu, W. Wang, "Highly coupled leaky surface acoustic wave on hetero acoustic layer structures based on ScAlN thin films with a c-axis tilt angle" *Japanese Journal of Applied Physics*, vol. 60, no. 3, p.031002, 2021.

[21] M. Hiebel, Fundamentals of vector network analysis, second edition, München, Germany: Rohde & Schwarz, ISBN: 978-3-939837-06-0, 2007.

[22] C. Heeg, Spin mechanics at radio frequencies, Diploma thesis, Dept. Phys., Tech. Univ. Munich, München, Germany, 2010 Available: https://www.wmi.badw.de/fileadmin/WMI/Publications/Heeg_Diplomarbeit_2010.pdf

[23] L. Dreher, M. Weiler, M. Pernpeintner, H. Huebl, R. Gross, M. S. Brandt, and S. T. B. Goennenwein, "Surface acoustic wave driven ferromagnetic resonance in nickel thin films: Theory and experiment", *Phys. Rev. B,* vol. 86, Issue 13, 134415, 2012, https://doi.org/10.1103/PhysRevB.86.134415